The Pennsylvania State University

The Graduate School

College of Earth and Mineral Sciences

SOURCE CHARACTERIZATION WITH ATMOSPHERIC BOUNDARY LAYER DEPTH

A Thesis in

Meteorology

by

Andrew J. Annunzio

Submitted in Partial Fulfillment
of the Requirements
for the Degree of

Master of Science

August 2008

The thesis of Andrew J. Annunzio was reviewed and approved* by the following:

Sue Ellen Haupt
Senior Research Associate, Applied Research Laboratory and
Associate Professor of Meteorology
Thesis Co-Advisor

George S. Young
Professor of Meteorology
Thesis Co-Advisor

John C. Wyngaard
Professor of Meteorology

William H. Brune
Head of the Department of Meteorology
Professor of Meteorology

*Signatures on file at the graduate school

ABSTRACT

Characterizing the source of a contaminant is a contemporary issue in atmospheric transport and dispersion modeling. In addition to the source parameters, it is also necessary to back-calculate meteorological forcing parameters because they govern the subsequent transport of a contaminant. One aspect that has not been addressed previously is ascertaining the height of the atmospheric boundary layer. The capping inversion at the top of the boundary layer traps the puff by reflecting contaminants back towards the surface, directly impacting surface concentrations. Because the depth of the atmospheric boundary layer varies with time of day, stability, and the horizontal and vertical wind, it is generally difficult to determine. In the Gaussian puff model, a rigid lid is added to the top of the boundary layer to reflect contaminants back towards the surface. From time dependent concentration observations of the puff a Genetic Algorithm characterizes the source strength and location, boundary layer height, wind speed, and wind direction. It is shown that the Genetic Algorithm can back-calculate all these parameters working solely from concentration observations.

Table of Contents

List of Tables

List of Figures

Acknowledgements

I would first like to thank my advisors for their help and guidance. I also thank the office of 402, especially 402 A for work breaks from time to time. I especially thank Yuki Kuroki, Luna Rodriguez, Kerrie Long, and Anke Beyer-Lout for their help and support. Lastly, and most importantly I would like to thank my parents and my girlfriend, Heather, for putting up with me for the past two years and taking my mind off school when I got too stressed.

Chapter 1: INTRODUCTION

The atmospheric boundary layer (ABL) is generally characterized as a turbulent region in the atmosphere. Turbulent flow differs from laminar flow as turbulence is much more efficient than molecular diffusion in transferring heat and momentum. Turbulence is enigmatic as well, with the many scales of motion and randomness of the flow field making the problem intractable so that exact analytic solutions cannot be formed without gross simplifications (Wyngaard, 2008). In the atmospheric boundary layer, turbulence is almost always present and scales of motion can range from around a millimeter to over a kilometer (Wyngaard, 2008). Because turbulent energy is negligible on the molecular scale (Batchelor, 1953), the Navier-Stokes equation set describes the evolution of the flow field for all the scales of motion. For incompressible flow in a non-rotating reference frame the momentum and continuity equations in the Navier-Stokes equation set are given by:

$$\frac{\partial \widetilde{u}_i}{\partial t} + \widetilde{u}_j \frac{\partial \widetilde{u}_i}{\partial x_j} = -\frac{1}{\rho_o}\frac{\partial \widetilde{p}}{\partial x_i} - g\delta_{i3} + \nu \frac{\partial^2 \widetilde{u}_i}{\partial x_j \partial x_j}$$

$$\frac{\partial \widetilde{u}_i}{\partial x_i} = \frac{\partial \widetilde{u}}{\partial x} + \frac{\partial \widetilde{v}}{\partial y} + \frac{\partial \widetilde{w}}{\partial z} = 0 \qquad (1)$$

where $\widetilde{u}_i$ is the three dimensional velocity field, $\widetilde{u}$, $\widetilde{v}$, and $\widetilde{w}$ are the horizontal, meridional, and vertical velocity components respectively, $\widetilde{p}$ is the pressure, g is the gravity constant, ρ_o represents the mean density, ν is the kinematic viscosity and δ_{i3} is the kronecker delta function. The tilde represents the full turbulent variable and is equal

to the mean plus fluctuating component of the variable in question. For instance the full variable for velocity is given by:

$$\widetilde{u}_i = U_i + u_i \tag{2}$$

where U_i denotes the mean and u_i denotes the fluctuating component of velocity (Wyngaard, 2008). In incompressible flow the density of the fluid is constant so in this simplified case the equations do not allow buoyancy forces to contribute to the evolution of the flow. Incompressible flows apply to an engineering setting without imposed gradients of temperature and density, and turbulent production is dominated by shear. In the atmospheric boundary layer, however, wind shear may no longer be the dominant mechanism, and buoyancy dominates turbulent production. Further, in a stably stratified boundary layer, variations in density dampen vertical motions and cause the turbulence to decay. To account for these small density variations in the atmosphere, (1) is modified such that density variations are neglected except when multiplied by gravity. Noting that density variations in the atmospheric boundary layer are generally caused by temperature and moisture variations one can substitute virtual temperature for density. Further, one can substitute virtual potential temperature for virtual temperature because the ratio of virtual temperature to its base state is equivalent to the ratio of virtual potential temperature to its base state. Then the momentum and continuity equations, known as the Boussenesq momentum and continuity equations, in a rotating reference frame are given by:

$$\frac{\partial \widetilde{u}_i}{\partial t} + \widetilde{u}_j \frac{\partial \widetilde{u}_i}{\partial x_j} = -\frac{\partial \widetilde{p}'}{\partial x_i} - 2\varepsilon_{ijk}\Omega_j \widetilde{u}_k + \frac{\widetilde{\theta}_v'}{\theta_o} g\delta_{i3} + \nu \frac{\partial^2 \widetilde{u}_i}{\partial x_j \partial x_j}$$

$$\frac{\partial \widetilde{u}_i}{\partial x_i} = \frac{\partial \widetilde{u}}{\partial x} + \frac{\partial \widetilde{v}}{\partial y} + \frac{\partial \widetilde{w}}{\partial z} = \frac{\widetilde{w}}{H_\rho} \approx 0 \qquad (3)$$

where H_ρ is the density scale height of the atmosphere, p' is the pressure deviation Ω_j is the Coriolis term, ε_{ijk} is the alternating tensor, and θ_v' is the temperature deviation from the base state θ_o. In the atmospheric boundary layer, the Reynolds number is generally high (greater than 10,000) as this region of the atmosphere is turbulent. Because the Reynolds number is large, the molecular diffusion term, $\nu \frac{\partial^2 \widetilde{u}_i}{\partial x_j \partial x_j}$, in (3) contributes little to the evolution of the flow and can be neglected. Analytical solutions to the Boussenesq equations are not possible in turbulent flow because there are no methods to solve a chaotic system of nonlinear PDE's (Batchelor, 1953). The range of scales present in a turbulent flow further complicates the goal of finding exact solutions. To combat this scale problem, one takes an ensemble average of the equations of motion. The averaging process requires splitting up the dependent variable into a mean and turbulent part and taking the ensemble average.

$$\overline{\frac{\partial (U_i + u_i)}{\partial t} + (U_j + u_j)\frac{\partial (U_i + u_i)}{\partial x_j}} = \overline{-\frac{\partial (P' + p')}{\partial x_i} - 2\varepsilon_{ijk}\Omega_j (U_k + u_k) + \frac{(\Theta_v' + \theta_v')}{\theta_o} g\delta_{i3}} \qquad (4)$$

where the over-bar denotes the averaging. The ensemble average is a linear operator and so commutes with other linear operators such as differentiation and addition. Making use of these averaging rules (4) becomes

$$\overline{\frac{\partial U_i}{\partial t}} + \overline{\frac{\partial u_i}{\partial x_i}} + \overline{U_j \frac{\partial U_i}{\partial x_j}} + \overline{U_j \frac{\partial u_i}{\partial x_j}} + \overline{u_j \frac{\partial U_i}{\partial x_j}} + \overline{u_j \frac{\partial u_i}{\partial x_j}} =$$
$$-\overline{\frac{\partial P'}{\partial x_i}} - \overline{\frac{\partial p'}{\partial x_i}} - 2\varepsilon_{ijk}\Omega_j \overline{U_k} - 2\varepsilon_{ijk}\Omega_j \overline{u_k} + \overline{\frac{\Theta_v'}{\theta_o}} g\delta_{i3} + \overline{\frac{\theta_v'}{\theta_o}} g\delta_{i3} \tag{5}$$

In a turbulent flow, the ensemble average of the fluctuating term is zero and the ensemble average of the mean is the mean. Implementing these averaging rules we obtain an equation for the mean evolution of velocity in turbulent flow.

$$\frac{\partial U_i}{\partial t} + U_j \frac{\partial U_i}{\partial x_j} + \overline{u_j \frac{\partial u_i}{\partial x_j}} = \frac{\partial P'}{\partial x_i} - 2\varepsilon_{ijk}\Omega_j U_k + \frac{\Theta_v'}{\theta_o} g\delta_{i3} \tag{6}$$

While this ensemble averaging alleviates the scale problem, a new term, $\overline{u_j \frac{\partial u_i}{\partial x_j}}$, arises from the averaging process. This new term in (6) is a covariance produced by averaging the nonlinear term, so one requires an evolution equation for this covariance in order to accurately describe the average flow. The covariance term is called a Reynolds stress, and scaling demonstrates that it contributes significantly to the evolution of the flow and cannot be neglected. Unfortunately, the evolution equation for the covariance yields a third order covariance so one needs an equation to describe its evolution in time. The same holds true for higher order covariance terms so determination of the evolution equation for these terms eventually yields an infinite set of equations. Therefore approximation to the covariance term is necessary at some time in this sequence, which degrades our ability to accurately describe the average flow field. A similar problem arises when one attempts to model the evolution of a scalar. In turbulent flow, the evolution of a scalar is given by:

$$\frac{\partial \tilde{c}}{\partial t} + \tilde{u}_i \frac{\partial \tilde{c}}{\partial x_i} = \gamma \frac{\partial^2 \tilde{c}}{\partial x_i \partial x_i} \tag{7}$$

where $\tilde{c}$ denotes concentration density and γ denotes the molecular diffusivity. While this equation is linear in $\tilde{c}$, one can see that it is coupled with the Navier-Stokes equation in the advection term. Therefore, in turbulent flow, this equation must be ensemble averaged as well. Let $\tilde{c} = C + c$ where C is the mean and c is the fluctuation, take the ensemble average of (7), and apply the averaging rules to obtain the mean evolution of a scalar in turbulent flow.

$$\frac{\partial C}{\partial t} + U_i \frac{\partial C}{\partial x_i} + \overline{u_i \frac{\partial c}{\partial x_i}} = \gamma \frac{\partial^2 C}{\partial x_i \partial x_i} \tag{8}$$

Away from solid boundaries, $\gamma \frac{\partial^2 C}{\partial x_i \partial x_i}$ contributes little to the evolution of the scalar and can be neglected. As with the equations of motion, the mean evolution of a scalar includes a covariance term, $\overline{u_i \frac{\partial c}{\partial x_i}}$. Accurately modeling the mean evolution of a scalar requires determination of an evolution equation for this covariance term, which leads to an infinite set of equations. The covariance term again contributes significantly to the mean evolution of the scalar, and therefore it cannot be neglected. The elusiveness of the stress term suggests that parameterizations to (8) are necessary.

1.1 Taylor Dispersion

In early efforts to describe turbulent flow, theoreticians attempted to describe turbulence in terms similar to those used for the movement of molecules. This mixing

length theory assumes that turbulence acts like molecular diffusion but on a larger scale, which suggests that the covariance term is related to larger scale gradients (Wyngaard, 2007). The covariance term is thus approximated using an eddy diffusivity; a technique which is known as first order closure. Using an eddy diffusivity closure for a simplified version of (8), G.I. Taylor produced one of the only analytic solutions for the evolution of a scalar in turbulent flow. To do so, however, some assumptions need to be invoked. First, the scalar equation must be decoupled from the flow field, which is achieved by assuming stationary, homogeneous turbulence. Further Taylor assumed a point source that is stationary and emits the scalar pollutant at a constant rate. To simplify the problem further, diffusion is limited to the vertical. These assumptions reduce (8) to:

$$U\frac{\partial C}{\partial x} = K_z \frac{\partial^2 C}{\partial z^2} \tag{9}$$

where K_z is the eddy diffusivity and U is the mean wind velocity. Equation (9) is a linear, partial differential equation, which is solved via a Fourier transform on an infinite domain. The solution is the Gaussian plume model:

$$C(x,z) = \frac{Q}{U\sigma_z (2\pi)^{\frac{1}{2}}} \exp\left(-\frac{(z-z_o)^2}{2\sigma_z^{\,2}} \right) \tag{10}$$

Where Q represents the strength of the stationary, continuous source release, z_o denotes the source height, and σ_z denotes the spread of the plume. In reality, (10) only exists in the ensemble mean, and is the result of the average of an infinite number of plume realizations in a turbulent flow. The σ denotes the spread of contaminant concentration.

This equation gives insight as to how turbulence will diffuse scalars if the turbulence is stationary and homogeneous. The squares of the σs are proportional to the mean square displacement of a fluid particle over a time interval t, which is related to the autocorrelation function (Wyngaard, 2007):

$$R(\tau) = \frac{\overline{w(t)w(t+\tau)}}{\overline{w^2}} \tag{11}$$

The range of the autocorrelation function is [-1, 1] and its value describes how the fluid particle "remembers" its velocity at a previous time (Wyngaard, 2008). For a short period after the initial velocity $w(t)$, the particle standard deviation of distance varies linearly with time, while for large time intervals the particle standard deviation grows according to the square root of time (Taylor, 1921). Lumley proved that in stationary, homogeneous turbulence the Lagrangian velocity is equal to the Eulerian velocity (Lumley, 1962). In terms of pollutant dispersion, initially after a release the σ increases linearly, and

$$\sigma_z = \frac{(\overline{w^2})^{\frac{1}{2}} x}{U} \tag{12}$$

when t is much smaller than the Lagrangian timescale where the Lagrangian timescale is determined by the length and velocity scales of the largest eddies. When t is much larger than the Lagrangian timescale,

$$\sigma_z = \left(\frac{(\overline{w^2}) x \tau_l}{U} \right)^{\frac{1}{2}} \tag{13}$$

and the σ increases parabolically (Wyngaard, 2008). Although, the mixing length assumption is a gross simplification of turbulence, the Gaussian plume equation and the statistical arguments by Taylor were big advancements in turbulence theory.

1.2 Puff vs. Plume Model

The Gaussian plume model can easily be extended to all three dimensions by assuming that turbulent diffusion is significant in all three directions. Also, including the time change term in equation (9) depends on our initial conditions. A continuous release assumes stationarity because the turbulence is assumed to be stationary and homogeneous. In this scenario, a point source emits continuously over an interval [0, T] producing a plume like that seen from a factory smokestack. Including the time change term allows modeling an instantaneous release where contaminant is released over a short time interval. The governing equation is given by:

$$\frac{\partial C}{\partial t} + U\frac{\partial C}{\partial x} - K_x\frac{\partial^2 C}{\partial x^2} - K_y\frac{\partial^2 C}{\partial y^2} - K_z\frac{\partial^2 C}{\partial z^2} = 0 \tag{13}$$

where the variables are the same as defined previously. One solves this equation in the same manner as (9) with a Fourier transform of the dependent variable. This is an infinite domain problem, and an initial condition must be specified to obtain the solution. Assuming an instantaneous release from some point source in the domain as the initial condition produces the Gaussian puff model given by:

$$C(x,y,z,t) = \frac{Q\Delta t}{U\sigma_x\sigma_y\sigma_z(2\pi)^{\frac{3}{2}}}\exp\left(-\frac{(x-(x_o+Ut))^2}{2\sigma_x{}^2}\right)\exp\left(-\frac{(y-y_o)^2}{2\sigma_y{}^2}\right)\exp\left(-\frac{(z-z_o)^2}{2\sigma_z{}^2}\right) \tag{14}$$

where Δt is the elapsed time of the release or length of emission and (x_o, y_o, z_o) is the three dimensional source location. In both the puff and plume case the σs have the same meaning and determine the spread the puff. The σs can be linear and/or parabolic as Taylor described, or can be empirically derived. The σs derived by McMullen are presented in Beychok and depend on the Pasquill stability class (McMullen, 1975). These values of σ give a more accurate description of plume growth for a Gaussian model and result from fitting a function to the Pasquill-Gifford curves. The Pasquill-Gifford curves result from the Prairie Grass experiments where observations were taken of surface concentration values of a contaminant under differing atmospheric conditions (Gifford, 1961). The σ s are prescribed by six different curves where each curve denotes a stability class ranging from an extremely unstable atmosphere to a stable atmosphere. More recent dispersion models abandon the stability class designation to eliminate air mass classification. This is done by relating the turbulent diffusion of a puff to the continuously varying stability parameter in the ABL, $\frac{z_i}{L}$, where z_i is the atmospheric boundary layer depth and L is the Monin-Obhukov length. However, Briggs gives an approximate mapping from the continuous varying stability parameter to the six stability classes. Roughly, an extremely unstable atmosphere is analogous to $-\frac{z_i}{L}$ greater than 100, and a moderately unstable atmosphere is analogous to $-\frac{z_i}{L}$ being less than 100 but greater than 20 and so forth (Briggs, 1988). Note that one can also better represent the dispersion of a puff or plume while maintaining low computational efforts by considering a varying eddy diffusivity, a logarithmic wind profile, or a dispersion model that more

accurately models the convective boundary layer (Weil, 1988). For this research, we use the traditional Gaussian derived by Taylor.

1.3 Dispersion Modeling

Modeling the release and spread of a contaminant is an important topic in homeland security as it is crucial to warn the public and to mitigate the effects of a contaminant in the case of a terrorist attack. Predicting contaminant concentration at ground level proves to be a very difficult task for several reasons. First, the initial conditions for the model are often unknown. When a sensor detects a contaminant in the field, source characteristics such as source location, strength of release, and the time of release may not be known. Secondly, even if source characteristics are known, meteorological parameters such as turbulence statistics and local mean wind speed and direction may not be accurately known. The mean wind speed and wind direction are undoubtedly the two most important meteorological factors in atmospheric transport, as contaminants move with the wind. As in previous work, both mean wind speed and direction are back-calculated in order to ascertain where the puff will be at a later time step (Allen et al, 2007; Long et al, 2008). While the mean wind speed and direction determine contaminant transport, these meteorological parameters are not sufficient to predict the areas of relative high and low concentration at the surface. The turbulence determines this, and the inability to accurately represent turbulence in a dispersion model limits our ability to predict these areas of high concentration that can be potentially lethal. Even if one could represent turbulence well in a model, the initial conditions for the flow must be known exactly for proper determination of the three dimensional velocity field

for a given realization. Flow characteristics are sensitive to initial conditions, and slightly improper initialization may produce vastly different results (Lorenz, 1963).

The earth's atmosphere can either be characterized as turbulent or non-turbulent. Near the surface of the earth the atmosphere is generally turbulent (unless the atmosphere is extremely stable) because of wind shear and positive buoyancy. In the absence of intense convective conditions, there is a thin boundary or inversion separating the turbulent air at the surface from the generally non-turbulent air above. If a contaminant release were to occur, it will most likely be in the turbulent part of the atmosphere where people live. Therefore, the inversion may also acts as a boundary between contaminated air below and clean air above in a contaminant release. For this reason, one can see that the depth of the boundary layer is an important parameter in atmospheric transport and dispersion. The stable layer at the top of the boundary layer prevents contaminants from escaping and downdrafts drive these contaminants back towards the surface, creating higher surface concentration values than what would occur if there was no boundary layer at all.

This work attempts to reduce uncertainty inherent in dispersion modeling by retrieving relevant meteorological parameters to atmospheric transport and dispersion as well as by retrieving source characteristics. To do so, we fit noisy concentration data to a trapped Gaussian puff model with a hybrid Genetic Algorithm (GA). The trapped Gaussian puff model extends (14) to include reflections from the ground and from the inversion representing in an ensemble averaged sense how the atmosphere lofts contaminants upward and downward. This is done mathematically by considering each reflection to be a virtual source centered outside of the domain (Csanady, 1973). This

work does not attempt to predict surface concentration values with a Gaussian model, but rather back-calculates important parameters needed to predict surface concentration values.

Chapter 2: RETRIEVING SOURCE CHARACTERISTICS AND METEROLOGICAL VARIABLES FROM CONTAMINANT CONCENTRATION

2.1 Introduction

The transport and dispersion of pollutants and harmful chemicals in the earth's atmosphere is of interest to many. Because most of these contaminants reside in the lower atmosphere where humans live, flows in the atmospheric boundary layer (ABL) are critically important. The ABL is generally turbulent, and therefore simulations of a contaminant release are plagued by uncertainty in the three dimensional velocity field. Irregular random motions can increase scalar gradients and thus may create areas of high concentration adjacent to areas of low concentration in the process of mixing the contaminant. Further, convection due to deviations in the surface heat balance creates turbulence and complicates the problem of ascertaining mean wind speed and wind direction to properly model the transport and dispersion of a contaminant. Also, the ABL is usually topped with a capping inversion that limits the domain of turbulence and also prevents contaminants from escaping into the free atmosphere and reflects them back towards the surface (Stull, 1988). By limiting the vertical extent to which contaminants can travel, the capping inversion creates higher concentration values at the surface and thus higher concentration values integrated over time as dosage.

This work utilizes surface concentration measurements to back-calculate the source characteristics of a release as well as the meteorological parameters relevant to atmospheric transport and dispersion. This is an extension of prior work where wind speed and direction were back-calculated along with the (x,y) source location, source strength, and time of release (Allen et al, 2007; Long et al, 2008). This work represents a

significant step, because the back-calculation includes atmospheric boundary layer depth as well.

2.2 Motivation

In homeland security and defense applications, the atmospheric transport and dispersion problem is twofold. First, the source characteristics, such as source location and source strength, of the contaminant are often unknown. In this case, before addressing where a contaminant puff will go, one must ascertain where it originated. Secondly, the atmospheric parameters that govern the dispersion of the contaminant must be diagnosed because atmospheric observations are generally sparse. While wind speed and wind direction are the most important meteorological parameters, the atmospheric boundary layer depth is also an important parameter when diagnosing surface concentrations (Holmes, 2006). The depth of the boundary layer, z_i, is the distance from the surface to the average top of the mixed layer (Stull, 1988). The impact of reflected contaminants on surface concentration depends on the depth of the boundary layer and atmospheric stability. A parameter that assesses the influence that a capping inversion has on the dispersion of a contaminant is the ventilation factor, given by the product of wind speed and boundary layer depth (Hsu, 2003). A shallow boundary layer coupled with calm winds implies low mixing volume and hence weak dispersion. Deep boundary layers with fast winds, on the other hand imply vigorous motions and high values of ventilation (Eagleman, 1996). Before using the ventilation factor, however, the height of the capping inversion and the average wind speed must be determined, hence their inclusion in the list of unknowns for the back-calculation problem.

2.3 Model Formulation

The goal of this study is to determine the contaminant source characteristics and meteorological parameters, including wind speed, wind direction, and boundary layer depth, in order to accurately model the transport and dispersion of the contaminant. The source location is assumed to be in the ABL, and thus below the inversion. In this study, unstable through neutral boundary layers are tested. Further, we deal with two types of problems: one with a stationary domain and one with a domain that varies with time in the vertical as the boundary layer grows. In the latter case, air is entrained into the boundary layer from the free atmosphere above as rising thermals penetrate through the capping inversion (Stull, 1988). In both cases the back-calculation is accomplished with an optimization technique. Such a calculation requires a robust optimization technique; therefore we implement a hybrid Genetic Algorithm (GA) for the task (Allen, 2006). Observed contaminant concentration must be available before any back-calculation can occur. Because real data is not readily available, a forward model computes concentration values at grid points in the domain. The GA optimizes the input parameters for the forward model to achieve the best match possible with the sensor monitored concentration data at grid points.

2.3.1 Forward model

For this problem we use an identical twin experiment where the model itself creates the observations (Daley, 1991). This approach is useful for technique development because it eliminates model errors as a source of uncertainty. The forward model chosen

to create synthetic data is the three dimensional trapped Gaussian puff model given by

$$C = \frac{Q\,\Delta t}{u\,\sigma_x \sigma_y \sigma_z (2\pi)^{\frac{3}{2}}} \exp\left(-\frac{(x_o - (x + ut))^2}{2\sigma_x^2}\right) \exp\left(-\frac{(y - y_o)^2}{2\sigma_y^2}\right) \times \left[\exp\left(-\frac{(z - z_o)^2}{2\sigma_z^2}\right) + \exp\left(-\frac{(z + z_o)^2}{2\sigma_z^2}\right) + \sum_{n=}^{N} \exp\left(-\frac{(z + z_o + 2nz_i)^2}{2\sigma_z^2}\right) + \exp\left(-\frac{(z - z_o + 2nz_i)^2}{2\sigma_z^2}\right) + \exp\left(-\frac{(z - z_o - 2nz_i)^2}{2\sigma_z^2}\right) + \exp\left(-\frac{(z + z_o - 2nz_i)^2}{2\sigma_z^2}\right)\right] \quad (15)$$

where σ_x, σ_y, and σ_z describe the horizontal and vertical spread of the puff, z_i is the boundary layer depth, z the height of the sensor, z_o is the height of the release, $Q\Delta t$ is the release rate over a time span Δt, u is the wind speed, N is the number of reflection terms included, and t is the time since the release. Experiments show that two or three reflection terms describe almost all of the dispersion; however, to avoid approximation errors we will use five reflection terms in creating the synthetic data (Beychok, 2005). The reflection of contaminants from of the capping inversion and the surface suggested by (15) occurs in the ensemble averaged sense. In reality rising thermals advect pollutants upward while downdrafts bring contaminants back towards the surface. Recycling of mass between these two branches of the convective circulations results in air parcels, and the contaminants they carry, alternately being lofted and lowered. If one takes an infinite number of realizations of a contaminant release in the turbulent ABL and averages them, the reflection terms of (15) would result. Therefore the reflection terms, just as the puff model itself, is valid in the ensemble average sense. The σs quantify the spread of the puff, and increase with distance from the source. The forward model computes the concentration at the sensors given "guesses" of the parameters to be

optimized. The hybrid GA optimizes the parameters by minimizing the sum over all grid points and time, of the squared difference between the concentration values in the synthetic data and the concentration values calculated from the current guess to the variables.

2.3.2 Domain Considerations

In (15) the vertical dispersion coefficient, σ_z, describes the vertical spread of the puff, and is given by

$$\sigma_z = \exp(I + J\ln(x) + K(\ln(x))^2) \tag{16}$$

The constants I, J, and K in (16) are functions of Pasquill stability classification and are determined by a look up table (Beychok, 2005). The three σs in (15) are not the σs determined by Taylor but are rather derived from the Pasquill-Gifford curves and take the form of (16) (Beychok, 2005). In general a more stable atmosphere yields smaller dispersion coefficients, thus limiting the spread of the puff. In contrast unstable conditions produce vigorous vertical motions causing the puff to spread very quickly: the dispersion coefficients are larger in this case. In very stable scenarios, retrieving atmospheric boundary layer depth is not possible because z_i approaches zero. In this case vertical motion everywhere is damped by stable stratification and contaminants do not travel far in the vertical. Therefore, retrieval of boundary layer depth is considered only for unstable through neutral atmospheric states. For a more stable atmosphere, reflected contaminants significantly influence surface concentration values further from the source, and one must consider an appropriate domain size for successful retrieval. If

the domain is not large enough, the puff will move out of the domain before reflected contaminants impact surface concentration values precluding back-calculation of boundary layer depth.

In order to determine the appropriate domain size we consider the Turner approximation

$$z_i = z_o + 2.15\sigma_z \tag{17}$$

to compute the horizontal distance at which the upper portion of the plume or puff is no longer Gaussian (Beychok, 2005). Turner developed the approximation for the plume model, but it applies to the puff model as well. In order to determine where contaminants reflecting from the base of the inversion impact surface concentrations, we extend Turner's equation to include a reflection from the source to the capping inversion, and back to the surface again.

$$2z_i - z_o = 2.15\sigma_z \tag{18}$$

If we substitute (16) into (18) and solve for x (see Appendix A for the complete derivation), we obtain the equation

$$x = \exp\left(-\frac{J}{2K} \pm \left(\left(\frac{I}{K} \ln\left(\frac{2z_i - z_o}{2.15}\right) - \frac{I}{K} \right) + \left(\frac{J}{2K} \right)^2 \right)^{\frac{1}{2}} \right) \tag{19}$$

Then, the distance x becomes the radius of our domain if we want reflected contaminants to significantly impact surface concentration by the time the puff moves out of the

domain. For less stable and neutral atmospheres this distance can be large, and therefore the distance x is taken as the domain radius.

2.3.3 The Hybrid Genetic Algorithm

The optimization technique employed for this work is a hybrid genetic algorithm: a combination of a genetic algorithm with the Nelder-Meade Downhill Simplex Algorithm. A genetic algorithm is a global optimization technique that is quite robust (Haupt and Haupt, 2004). A GA utilizes the natural selection process where the list of parameters are called chromosomes. At each iteration, the GA keeps and blends the best chromosomes and discards the worst chromosomes. Then, new chromosomes are randomly selected for possible mating if they are deemed fit enough (Haupt and Haupt, 2004). The mating scheme used here blends the variables instead of using the more standard single point crossover. A single point crossover results in switching a chromosome between two parents, while blending results from a linear recombination of the chromosome from both parents (Haupt and Haupt, 2004). The cost function employed is logarithmic and is given by:

$$\frac{\sum_{t=1}^{5}\left(\sum_{s=1}^{N_{sensor}}(\log_{10}(aC_s+\varepsilon)-\log_{10}(aR_s+\varepsilon))^2\right)^{\frac{1}{2}}}{\sum_{t=1}^{5}(\sum_{s=1}^{N_s}(\log_{10}(aR_s+\varepsilon))^2)^{\frac{1}{2}}} \tag{20}$$

where C_s is the concentration value given by placing current guesses to the variables into (15) and R_s is the sensor concentration value from the identical twin experiment. The constant ε is placed in the logarithm to avoid taking the logarithm of zero and is a scale

factor. The GA is the workhorse in the optimization problem and explores the whole solution space to locate the basin that holds the global minimum. After the GA locates the appropriate basin, the Nelder-Meade Downhill Simplex Algorithm takes over and quickly cascades down the basin to the global minimum (Allen et al, 2007; Long et al, 2008).

2.3.4 Testing the model

In the identical twin experiment the "truth" data is computed with the source location set at (0.0, 0.0) m in the (x,y) domain, the source strength is 1.0 kg, while the source height, $z_{release}$, is allowed two different values in different runs: 1 m and 50 m, and we allow the GA to search between 0 m and 1000 m. For the meteorological parameters, the mean wind speed is appropriate to the stability of the atmosphere, and the average wind direction is fixed at 180 degrees. The boundary layer depth is allowed to vary between 0 m and 4000 m, while the hybrid GA searches for a boundary layer depth between 0 m and 5000 m. We also vary stability by changing how the dispersion coefficients evolve in time. It is unnecessary to retrieve boundary layer depth in a stable atmosphere, because the boundary layer depth approaches zero. We employ an 8×8 sensor domain with five time steps during each puff simulation. For this research, we consider 50 runs for each back-calculation and take the median of the ensemble to obtain the final solution. Each ensemble simulation uses a different set of randomly selected initial values.

There are several objectives for our numerical experiments. First, we want to ascertain how many reflection terms are needed in order for the GA to converge to a

solution for a simple four parameter model where the unknowns are source height, source strength, boundary layer depth and wind direction. Second, we consider back-calculation during steady conditions when the boundary layer depth can be approximated as stationary. Invoking the steady state condition we determine a threshold for noise that the model can withstand before back-calculation for all parameters becomes unachievable. Lastly, we consider retrieval during unsteady conditions such as in the morning or early afternoon when the boundary layer is growing by entrainment of air from the free atmosphere.

2.4 Results

2.4.1 Retrieval with a Constant Boundary Layer Depth

The first mission of this research is to test the retrieval algorithm under conditions where the boundary layer depth remains constant with time. The mean boundary layer depth resides in the entrainment zone, whose existence results from updrafts mixing free atmosphere air into the boundary layer (Stull, 1988). A stationary boundary layer depth does not mean that the top of the mixed layer stays at a constant height. By stationarity we imply that the boundary layer attains its maximum depth and is growing slowly, or that the run time of the model is short such that boundary layer depth barely increases, or an increase in boundary layer depth is compensated equally by subsidence. The initial mass of a contaminant is conserved throughout the simulation, as contaminants are assumed to be confined to the region below the capping inversion. If z_i increases then anywhere the contaminant exists becomes part of the boundary layer for the purposes of this study.

2.4.1a Four Parameter Sensitivity Test

This sensitivity test yields the number of reflection terms necessary for successful back-calculation when considering a simple four parameter model. The parameters in question are wind direction, source strength, boundary layer depth, and source height; and the back-calculation is done for the four different atmospheric states studied here. We compute skill scores to assess the accuracy of the back-calculation. A skill score is determined for each variable based on the final solution found by the Nelder-Meade Downhill Simplex Algorithm. These individual skill scores are added together and divided by the number of parameters providing the "skill" of the back-calculation. A skill score greater than 0.1 implies a less successful retrieval and a skill score less than 0.1 implies a quite successful retrieval. It is of note that, for this study, we kept the GA configuration constant with a 320 population size, 80 iterations, and a 0.02 mutation rate for each stability class and number of reflection terms. The GA configuration used provides very good results with little computational cost for the four parameter model. As reflection terms are removed from the back-calculation the run time decreases because the GA is fitting the concentration values to a truncated version of the trapped Gaussian puff model. We could have added more iterations to improve results when the GA fits a model with fewer reflection terms, but we wanted to test the sensitivity of the back-calculation to the number of reflection terms.

Figure 1 contours skill scores for a 1 m source height and for all types of atmospheric conditions tested. The sensitivity test for an extremely unstable atmosphere presents some interesting results. When the atmosphere is very unstable and the boundary layer depth is

below 1000 m, the back-calculation is successful for any number of reflection terms. As the depth of the boundary layer increases, more reflection terms are necessary to accurately ascertain all four parameters in an extremely unstable atmosphere. For a neutral atmosphere, the back-calculation is successful for all boundary layer depths considered when two or more reflections terms are included. The back-calculation for a moderately unstable atmosphere yielded skill scores greater than 0.1 when two and three reflection terms are considered, while for a less unstable atmosphere results are always successful when three or more reflection term are considered. The unsuccessful results in these scenarios are attributed to the model finding a source height of 0 m instead of 1 m. The model finds an inaccurate source height in that case because the GA configuration is not sufficient to find the appropriate solution basin. If we adjust the GA configuration such that it is more robust then the appropriate source height is found, but for reasons mentioned above we keep the GA configuration constant for this study.

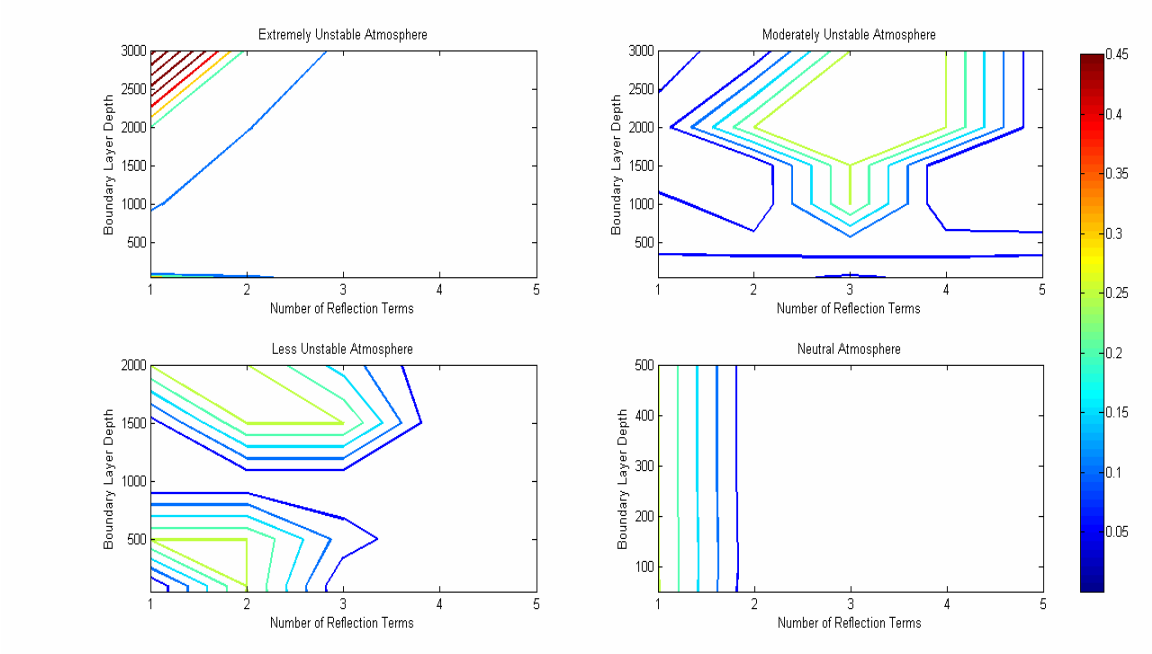

Figure 1: Contoured skill scores for the four parameter sensitivity test for a 50 m source height

When a 50 m source height is considered results improve. Figure 2 contours skill scores for an extremely unstable, moderately unstable, less unstable, and neutral atmosphere for a 50 m source height. Back-calculation is now successful for almost all boundary layer depths no matter the number of reflection terms for all atmospheric conditions considered except for the extremely unstable case; however, results are better when more reflection terms are included. The drastic decrease in skill scores for a moderately unstable atmosphere and a less unstable atmosphere is attributed to the hybrid GA correctly retrieving the source height. Given the same configuration, the model finds source height with greater ease when it is further away from the surface. For the 50 m release, an extremely unstable atmosphere and a neutral atmosphere yield nearly the same results as for the 1 meter release.

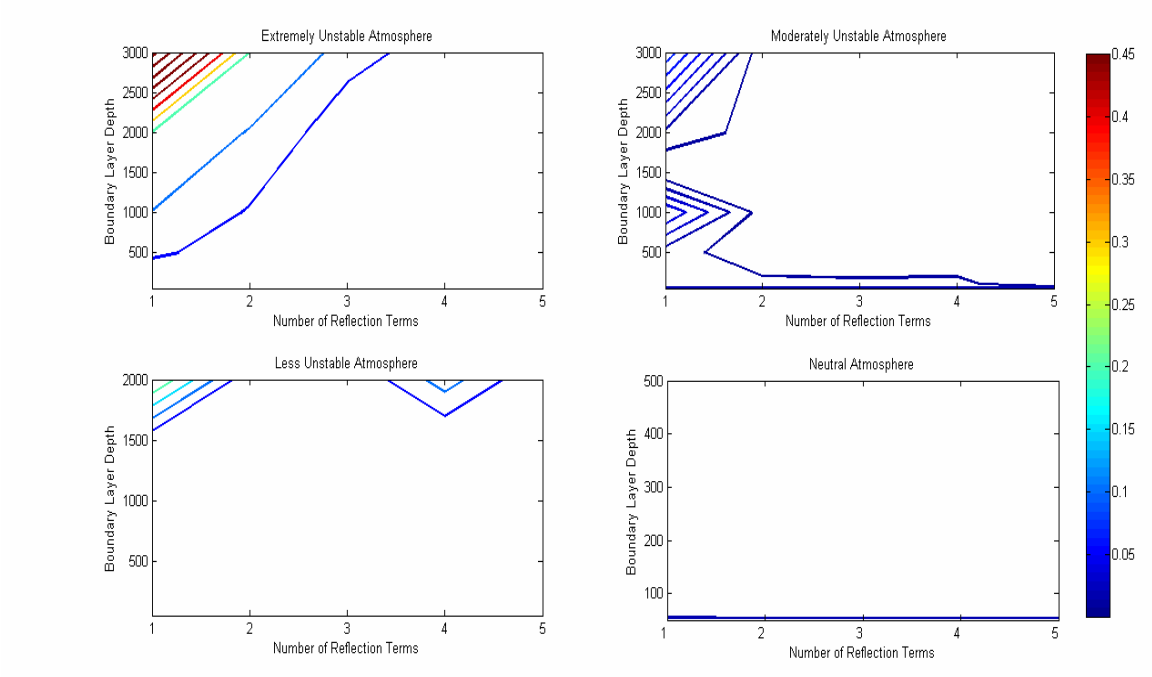

Figure 2: Contoured skill scores for the four parameter sensitivity test for a 50 m source height

2.4.1b Six Parameter Noise Test

Because observations are typically noisy, we consider how much noise the model can handle before back-calculation becomes unsuccessful. In the four parameter model, initial runs including noise illustrated that this model could handle moderate amounts of noise (not shown). Because we want to test the robustness of the GA in the presence of noise, we increase the number or unknowns, and move beyond the four parameter model. Before considering any noise test, we must determine how many parameters the hybrid GA can back-calculate successfully with no noise. In previous research it was determined that back-calculation is successful for a six parameter model where the parameters are (x,y) source location, source strength, wind direction, wind speed, and time of release (Long, 2008). Because the six parameter model was successful when release time was an unknown instead of boundary layer depth we will first see if the hybrid GA can back-calculate seven parameters. In this research it is assumed that release time is known, hence for the seven parameter model boundary layer depth and source height are substituted for time as unknowns. Figures 3 and 4 display the results for the seven parameter model when the source height is 1 m and 50 m respectively.

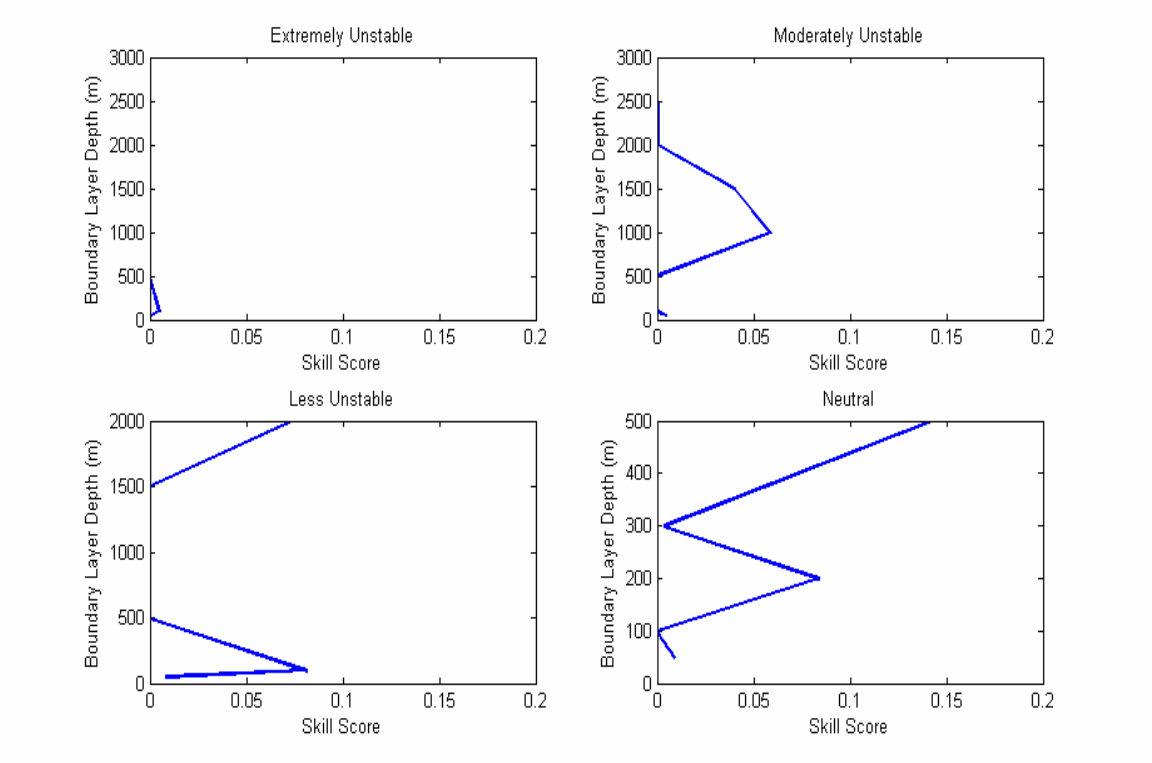

Figure 3: Skill scores for the seven parameter model for a 1 m source height

Both figures illustrate that retrieval is generally successful for an extremely unstable and moderately unstable atmosphere, which results from a smaller domain, and hence, a smaller solution space for the hybrid GA to work with. Retrieval becomes more difficult for a less unstable atmosphere and even more difficult for a neutral atmosphere as the boundary layer depth increases. The less successful retrieval results from inability to accurately retrieve source height; therefore we exclude source height in the subsequent back-calculations. The ability of the GA to successfully back-calculate the unknowns is highly dependent on the GA configuration. The configuration adopted for the seven parameter model is 1200 iterations, 180 population size, and a 0.02 mutation rate. The only other configuration that yields marginal success in back-calculation for the seven

parameter model is 720 iterations, 360 population size, and a 0.02 mutation rate; however, this configuration can only retrieve source height when there is little noise.

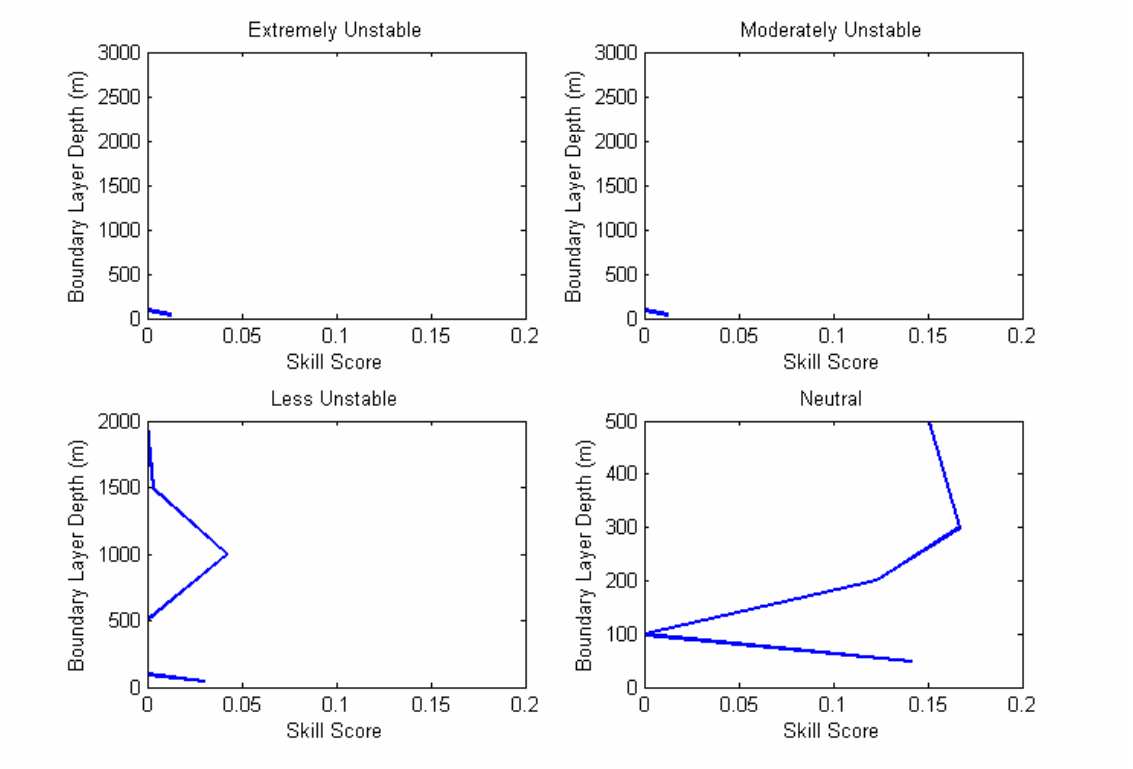

Figure 4: Skill scores for the seven parameter model for a 50 m source height

Because retrieval of all seven parameters is not successful when the atmospheric stability is neutral and the environment is noiseless, we consider a six parameter model for the noise test. A lesson learned from the seven parameter model is that retrieval becomes difficult in a neutral atmosphere when the boundary layer depth is greater than 200 meters because the domain becomes very large. This same idea applies to the six parameter model because the (x,y) source location is unknown and hence the GA has to search a large solution space. Therefore, we must determine the proper GA configuration for retrieval of the six parameters during neutral atmospheric conditions in order to

achieve successful back-calculation during all atmospheric conditions considered. In order to determine this configuration, we test retrieving the unknowns when the boundary layer depth is 400 m and the signal-to-noise ratio is infinite. The median skill score and minimum cost function is found by taking the median of both in an ensemble of ten runs. It is of note that the sufficient configuration for the six parameter model is not sufficient for the seven parameter model and vice versa. Figure 5 displays the skill scores for different GA configurations.

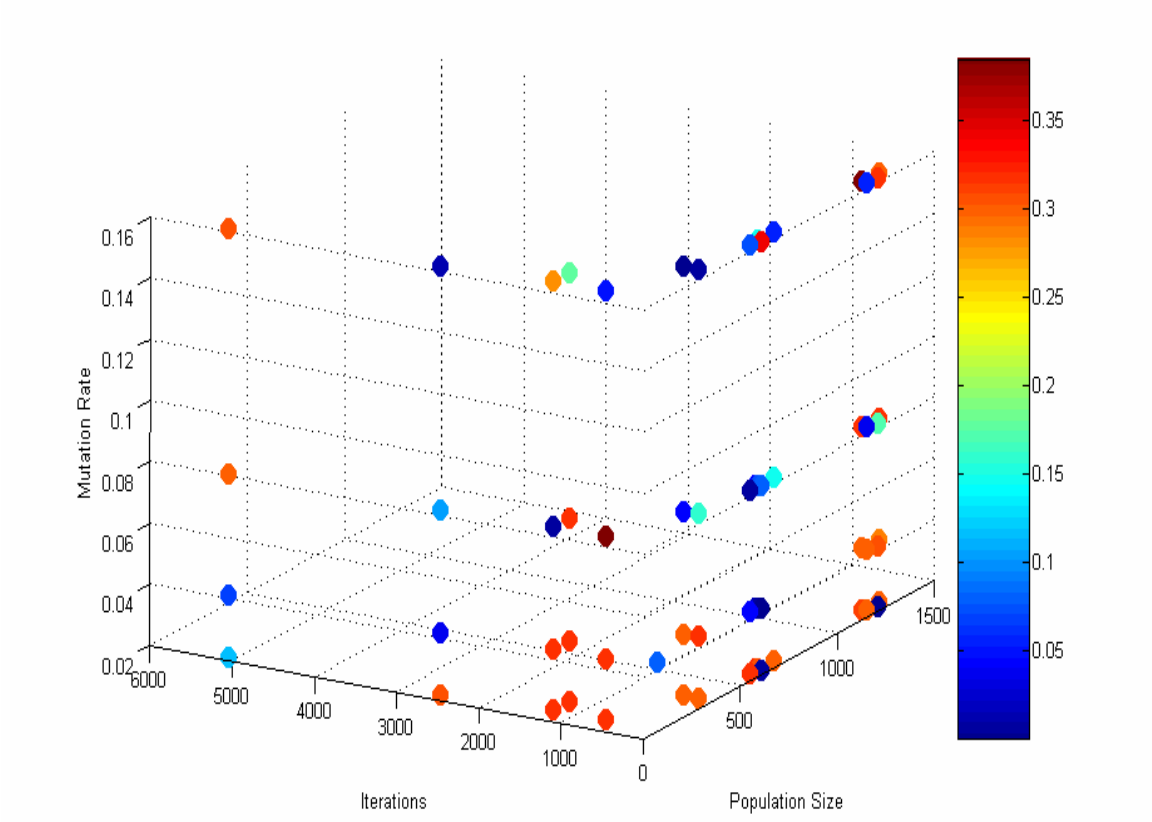

Figure 5: Median skill scores for several GA configurations

Generally, a medium to large population size with a small number of iterations yields the lowest skill scores while a small population with a moderate number of iterations yields the highest skill scores. It is also necessary to observe the convergence properties of the GA configuration to investigate if the hybrid GA is getting caught in local minima. Figure 6 displays the median of the value of the natural log of the cost function in the ensemble for GA configurations tested. The figure illustrates that the hybrid GA indeed

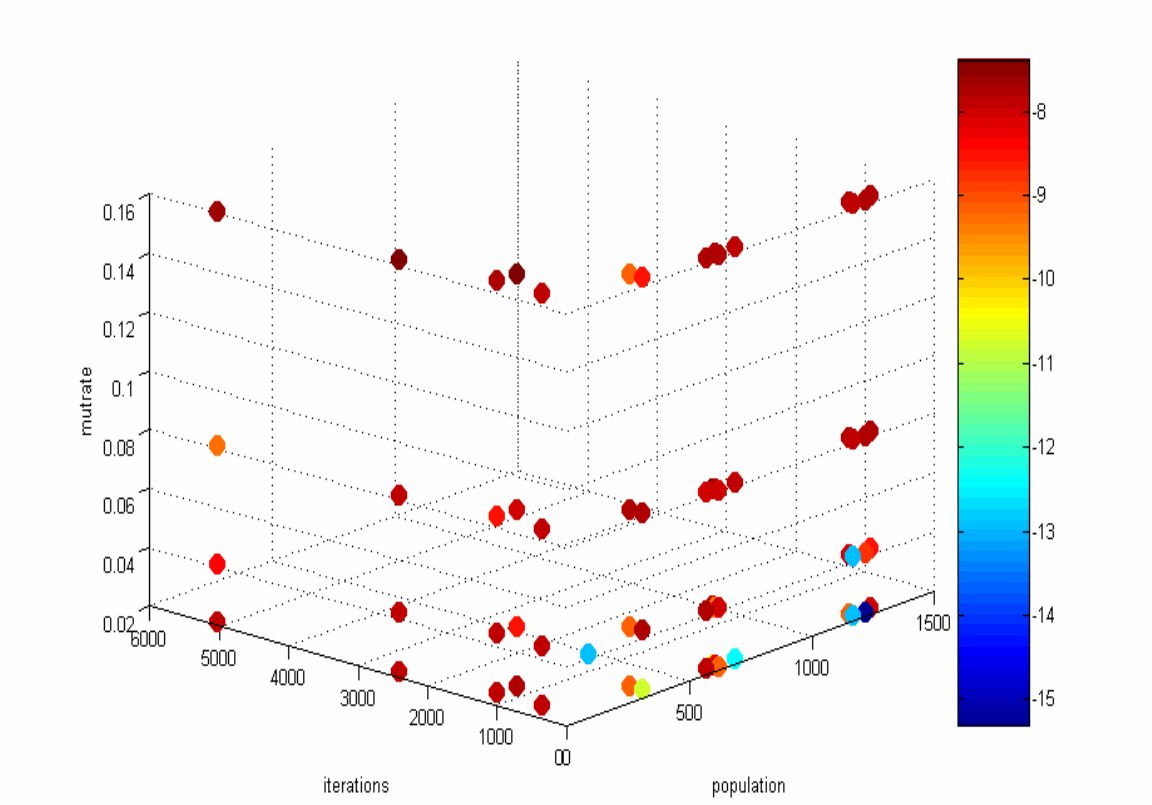

Figure 6: Logarithm of the median value of the cost function for several GA configurations

is getting caught in a local minimum and converging to an incorrect solution for almost all of the configurations tested. The configurations that do not get caught in this improper solution basin consist of a large population size, a small number of iterations, and low mutation rate. Therefore, for the six parameter model we consider two GA configurations: the first a population size of 640, a mutation rate of .04, and 80 iterations

and second a population size of 1200, a mutation rate of 0.02 or 0.04, and 80 iterations. Initially the first configuration is employed for the back-calculation; however, if this configuration yields an unsuccessful result the second GA configuration is employed. With the new GA configurations, we test the six parameter model with no noise in order to compare these results with those of the seven parameter model. Figures 7 and 8 plot skill scores vs. boundary layer depth for the different atmospheric states tested when the source height is 1 m and 50 m respectively.

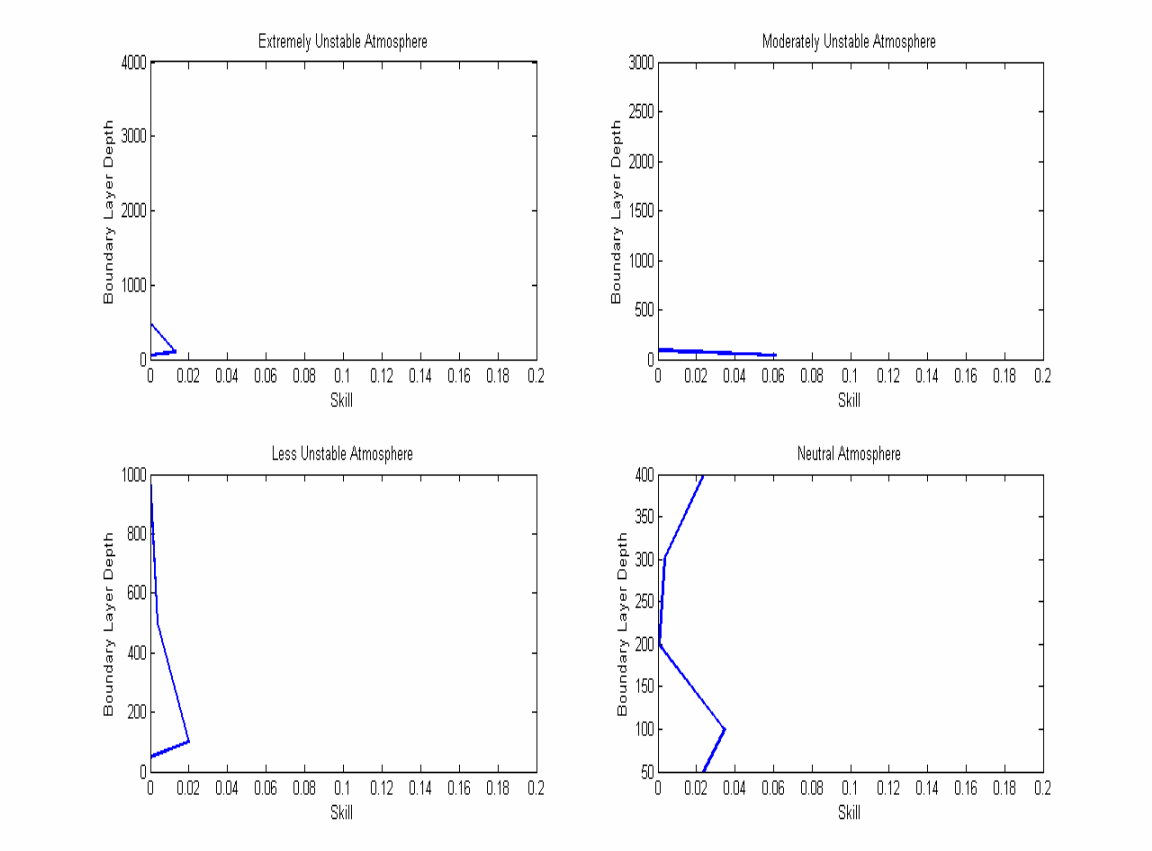

Figure 7: Six parameter results without noise for a 1 m source height

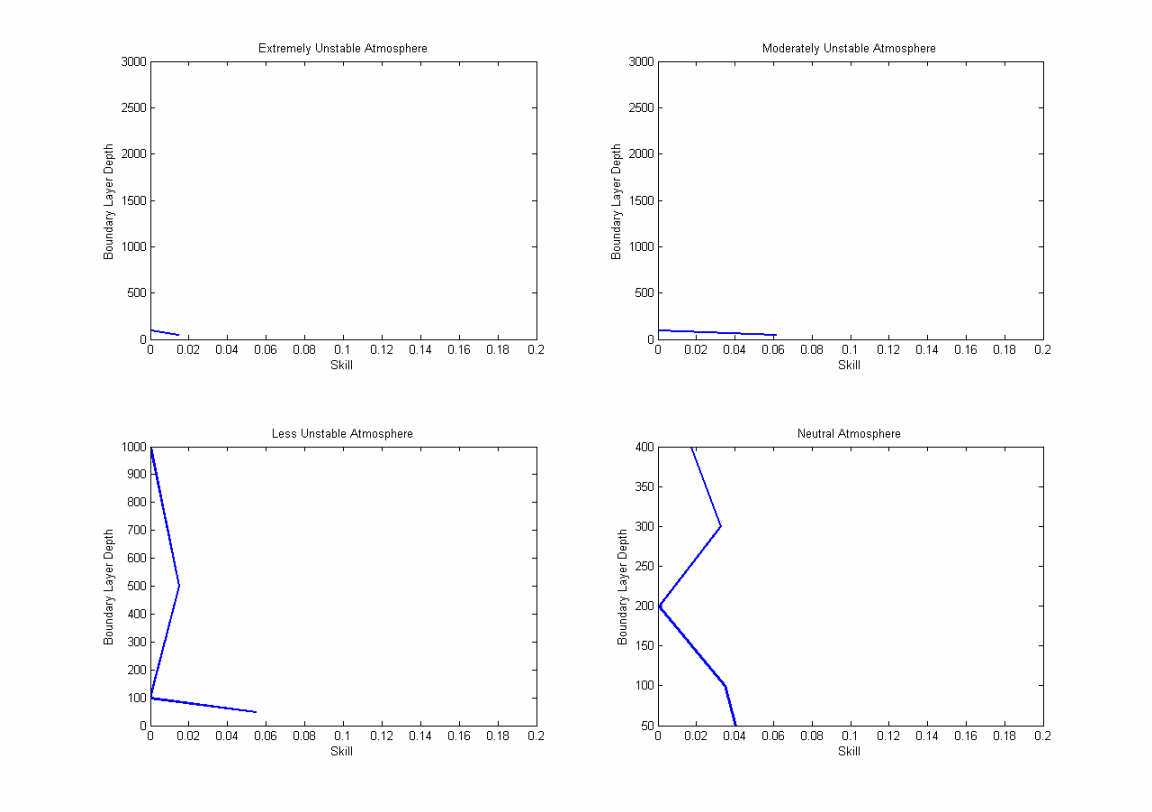

Figure 8: Six parameter results without noise for a 50 m source height

These figures illustrate that when the atmosphere is neutral the back-calculation is successful for all boundary layer depths considered. As expected, because the back-calculation is successful for a neutral atmosphere, retrieval is also successful when the atmosphere is unstable.

Because the back-calculation is successful for all boundary layer depths and atmospheric stability states considered, we can then test how much noise the model can handle before retrieval is unsuccessful. The noise added to the model is additive clipped Gaussian white noise, and the signal-to-noise ratios tested are infinite, 100, 50, 10, 5, and

2. Figures 9 and 10 contour skill scores for an extremely unstable and a neutral atmosphere when the source height is 1 m and a 50 m respectively. In these figures, the moderately unstable and slightly unstable results are omitted as both plots do not reveal new information.

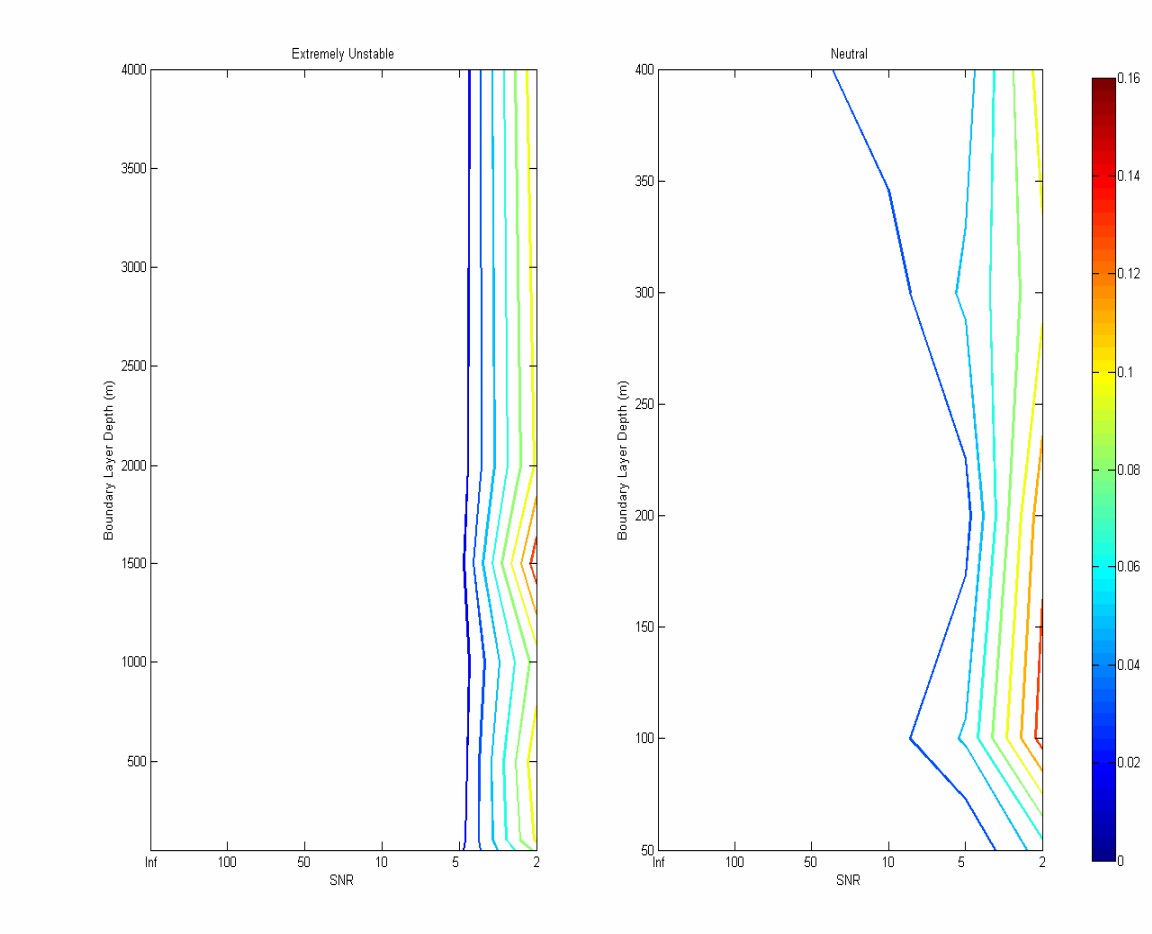

Figure 9: Skill scores for the six parameter noise test for a 1 m source height

When the source height is 1 m the back-calculation is successful in both an extremely unstable and neutral atmosphere for all boundary layer depths tested when the signal to noise ratio is greater than five. Results are still more accurate in an unstable atmosphere, however, as skill scores for all boundary layer depths in the unstable case

remain below .02 until the SNR is five while in the neutral case the skill scores remain below .06 until the SNR is five.

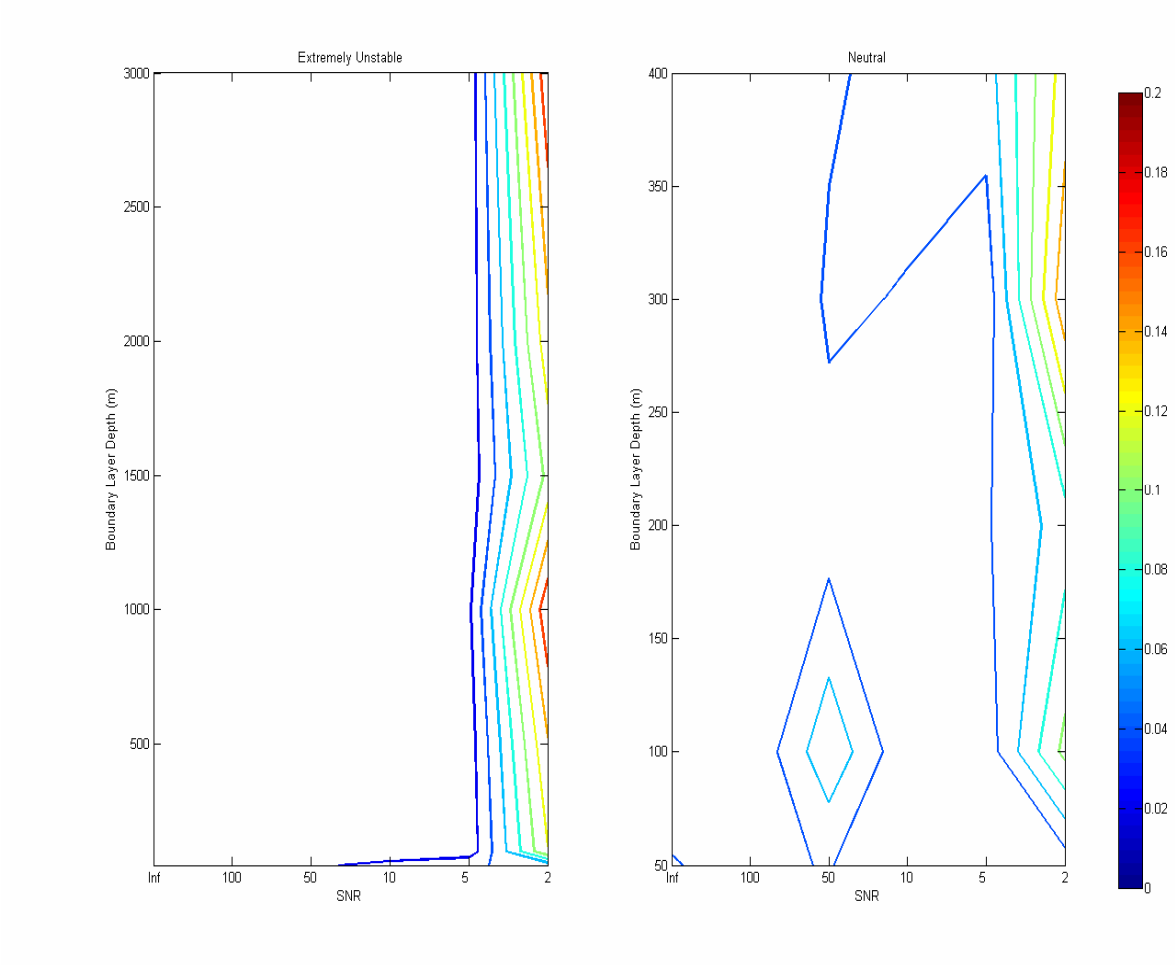

Figure 10: Skill scores for the six parameter noise test for a 50 m source height

When the source height is moved to 50 m, results are similar. In fact, figure 10 is very similar to figure 9, except with some subtle differences. One difference is that in a neutral atmosphere retrieval is still successful when the SNR is two where the source height and boundary layer depth are equal. In general these two figures show that the six parameter model can successfully back-calculate the unknowns when observations are corrupted by low to moderate amounts of noise.

2.4.2 Retrieval under Non-Stationary Conditions

The previous experiments invoke the assumption that the boundary layer depth does not change with time; however this assumption is not always valid. For instance, the boundary layer depth is assumed to be stationary at 100 meters for an extremely unstable atmosphere, which is only applicable in the morning before thermals completely obliterate the nocturnal inversion. Obviously, the inversion height does not remain constant at this time of day because rising thermals penetrate the inversion, entraining air from the residual layer and thus increasing the depth of the boundary layer. We can consider a constant boundary layer depth at this time, because the domain size is small, and thus, advection time and the corresponding time for inversion rise is short. Vigorous motions in a small vertical domain imply that reflected contaminants significantly impact surface concentration values very close to the source, as a result of Turner's approximation given by equation (19). Equation (19) indicates that reflected contaminants influence surface concentration values a couple hundred meters from the source. Dividing this quantity by wind speed yields the time in seconds before surface concentration is augmented by reflected concentration; a time period of less than a minute. Therefore, as long as the nocturnal inversion is not completely destroyed by energetic parcels of air, a stationary boundary layer depth is not a bad assumption. The same argument applies after the nocturnal inversion dissipates and the domain stretches to the top of the previous day's residual layer that becomes the mixing layer. At this time the boundary layer depth is increasing at a rate similar to that seen in early morning, and this rate is equivalent to the entrainment velocity, which is near 0.02 m/s. This suggests

that the only time period (besides early evening) when stationarity is a bad assumption is just after the nocturnal inversion breaks and the boundary layer depth increases just as fast as the thermals rise where a Gaussian dispersion model is no longer applicable as the back-calculating model.

In spite of this argument, we will consider retrieval of the six parameters when the height of the capping inversion is not stationary. The back-calculation is done in the same manner as before, except that in the trapped Gaussian puff model the boundary layer depth is allowed to increase linearly with time. This test is done when the atmosphere is extremely unstable since rising thermals are most vigorous and entrainment velocities are the greatest. When considering a boundary layer depth that is increasing with time, the total mass of the puff is still conserved as long as venting does not occur as it does with cumulus clouds. Thermals penetrate through the capping inversion into the free atmosphere, which causes free atmosphere air to be entrained in, but the thermals then sink back down below the inversion. No contaminants escape into the free atmosphere as the air above the boundary layer is generally non-turbulent, and thus there is no mechanism to disperse pollutants horizontally or vertically.

Non-stationary conditions are considered for two different unstable scenarios. The first scenario considers an extremely unstable atmosphere early in the morning before the nocturnal inversion dissipates. The initial boundary layer depth is 100 m, and the depth increases linearly in direct proportion to the entrainment velocity, which is set at 0.02 m/s. For this scenario, observation data is available every 48 s for five time steps, creating a total simulated run time of 240 seconds. Therefore, the boundary layer depth increases by 4.8 m throughout the run, and the mean boundary layer depth is 102.4 m.

Table 1 illustrates that retrieval is still successful as an unstable boundary layer grows by entrainment. The skill scores in Table 1 are the total skill scores for all six parameters while the Mean Absolute Error is only for boundary layer depth. Those skill scores are all quite good, even when the SNR is as low as 2. It is more instructive to note the median retrieval of boundary layer depth and its error in the last two columns. The error becomes significant when the SNR equals 5 and quite large for a SNR of 2.

Table 1: Success of boundary layer depth retrieval for a growing boundary layer whose initial depth is 100 m

SNR	Median Skill Score	Median Retrieved Boundary Layer Depth	Mean Absolute Error For Boundary layer Depth Retrieval
Inf	0.0019	102.09	0.31
100	0.0022	102.04	0.37
50	0.0022	102.00	0.40
10	0.0034	102.01	0.39
5	0.0060	104.38	1.98
2	0.0777	151.80	49.40

We also consider retrieval in an unstable atmosphere around mid-to late-afternoon. For this scenario, the boundary layer depth is initially set at 1000 m and grows according to the same entrainment velocity. The time to maximum height increases to 880 seconds, implying that the final boundary layer depth is 1017.6 m and the average

boundary layer depth is 1008.8 m. Table 2 displays the results for this scenario. Again, the skill scores reveal that the back-calculation is quite good even when the SNR is 2. The absolute error is generally greater than when the boundary layer depth is initially 100 m, except for when the SNR is 2.

Table 2: Success of boundary layer depth retrieval for a growing boundary layer whose initial depth is 1000 m

SNR	Median Skill Score	Median Retrieved Boundary Layer Depth	Mean Absolute Error For Boundary Layer Depth Retrieval
Inf	.00018	1008.80	0.00
100	.00065	1007.55	1.25
50	.00076	1008.00	0.80
10	.00325	1007.00	1.80
5	.00680	1021.50	12.7
2	.09225	1037.40	28.6

2.5 Conclusions

When back-calculating boundary layer depth as well as many other parameters in the Gaussian puff equation, many factors need to be taken into account. First, we need to make sure that the domain is the right size for the appropriate stability class. If the domain is too small, then contaminants reflected off the base of the capping inversion will not significantly affect surface concentration values, making back-calculation impossible. Second, with a more stable atmosphere and a larger domain size, we lose the

dense network of sensors, and the GA must work with the same amount of information over a much larger area. We have shown that there is a very delicate balance between the amount of information needed and the proper configuration for back-calculation. The difficulty of the back-calculation is greatest when the atmosphere is neutral, and the retrieval becomes much less difficult as the atmosphere becomes more unstable. In general, the more unstable the atmosphere the easier the back-calculation because of increased vertical transport and reflected contaminants increasing surface concentration values closer to the source.

Assuming a stationary boundary layer depth is valid if the back-calculation is done over a short time interval or if back-calculation is considered during midday or when the atmosphere is not unstable. When the atmosphere is more unstable, however, the assumption of stationarity is not as valid because rising thermals are penetrating the capping inversion and entraining air from the free atmosphere, causing the boundary layer depth to increase. Therefore we tested retrieval when the boundary layer depth is growing at its maximum rate (not considering the case when the nocturnal inversion breaks). This work has only considered a trapped Gaussian puff model in an identical twin experiment.

Further work will increase the complexity of the dispersion model, especially during an extremely unstable atmosphere where the locus of maximum concentration rises or falls dependent on the height of the source. To account for the vertical displacement of the puff will require considering an alternative dispersion model that requires the puff to be non-Gaussian in the vertical (Weil, 1988). Further work will also

consider retrieval without an identical twin experiment where surface concentration values are given from real data or simulated data.

Chapter 3: FINAL CONCLUSIONS

This thesis has looked at reducing the uncertainty present in modeling the release of a contaminant in turbulent flow by back-calculating source characteristics and meteorological parameters such as mean wind speed, wind direction, and boundary layer depth as well as source parameters. The back-calculation is accomplished by fitting contaminant concentration to a trapped Gaussian puff model with a hybrid GA. The robustness of the model is tested by the addition of noise and it found that the hybrid GA can successful back-calculate the six parameters in a low noise environment.

In future work we continue to combat the uncertainty problem by utilizing available data with methods such as Multisensor Data Fusion and Data Assimilation. These methods differ from the GA back-calculation as these methods update dynamical equations with observations in order to better predict the contaminant distribution instead of back-calculating parameters. We will do an analytic comparison of the two by assuming a contaminant release in stationary, homogeneous turbulence. After the comparison we will explore this problem further by relaxing the assumption of stationary, homogeneous turbulence which will require numerics. Also, we will consider merging the two methods with the GA back-calculation in hope to further reduce the uncertainty inherent in a contaminant release in turbulent flow. Therefore we will continue to address the uncertainty problem in hopes of better predicting surface concentration values if a contaminant release were to occur.

Appendix: Derivation of the distance where reflection terms begin to significantly impact surface concentrations.

We start with the extended Turner approximation:

$$2z_i - z_o = 2.15\sigma_z \tag{A.1}$$

where

$$\sigma_z = \exp(I + J(\ln(x)) + K(\ln(x))^2) \tag{A.2}$$

The horizontal distance is found by substituting (A.2) into (A.1) and solving for x.

$$2z_i - z_o = 2.15\exp(I + J(\ln(x)) + K(\ln(x))^2) \tag{A.3}$$

Dividing by (2.15) and taking the natural logarithm of both sides gives

$$\ln(\frac{2z_i - z_o}{2.15}) = I + J(\ln(x)) + K(\ln(x))^2 \tag{A.4}$$

We then bring I to the left hand side and divide by K

$$\left(\frac{1}{K}\ln(\frac{2z_i - z_o}{2.15}) - \frac{I}{K}\right) = \frac{J}{K}(\ln(x)) + (\ln(x))^2 \tag{A.5}$$

Completing the square yields

$$\left(\frac{1}{K}\ln(\frac{2z_i - z_o}{2.15}) - \frac{I}{K}\right) = -(\frac{J}{2K})^2 + \left((\frac{J}{2K})^2 + \frac{J}{K}(\ln(x)) + (\ln(x))^2\right) \tag{A.6}$$

which is equivalent to

$$\left(\frac{1}{K}\ln(\frac{2z_i - z_o}{2.15}) - \frac{I}{K}\right) + (\frac{J}{2K})^2 = \left(\frac{J}{2K} + (\ln(x))\right)^2 \tag{A.7}$$

Then one can easily solve for x, giving the expression

$$x = \exp\left(-(\frac{J}{2K})^2 \pm \left(\left(\frac{1}{K}\ln(\frac{2z_i - z_o}{2.15}) - \frac{I}{K}\right) + (\frac{J}{2K})^2\right)^{\frac{1}{2}}\right) \tag{A.8}$$

References

Allen, C.T., G.S. Young, and S.E. Haupt, 2006a: Improving Pollutant Source Characterization by Optimizing Meteorological Data with a Genetic Algorithm, *Atmospheric Environment,* **41**, 2283-2289.

Allen, C.T., S.E. Haupt., G.S. Young, 2007: Source Characterization with a Receptor/Dispersion Model Coupled with a Genetic Algorithm *Journal of Applied Meteorology and Climatology*, **46**, 273-287.

Batchelor, G.K., 1953: *The Theory of Homogeneous Turbulence.* Cambridge University Press, New York, NY, 195 pp.

Briggs, G.A., Analysis of diffusion field experiments. *Lectures on Air Pollution Modeling,* A. Venkatram and J.C. Wyngaard, Eds., Amer. Meter. Soc. 167-227.

Beychok, M.R., 2005: *Fundamentals of Stack Gas Dispersion, 4th Edition.* Irvine, CA, 201 pp.

Csanady, G.T., 1973: *Turbulent diffusion in the Environment.* D. Reidel Publishing Company, Dordrecht, Holland, 248 pp.

Daley, R., 1991: *Atmospheric Data Analysis*. Cambridge University Press, New York, NY, 457 pp.

Eagleman, J.R., 1996: *Air Pollution Meteorology 2nd Edition*. Trimedia Publishing Co., 258 pp.

Gifford, F.A., 1961: Use of Routine Meteorological Observations for Estimating Atmospheric Dispersion, Nuclear Safety, 2(4): 47-51.

Haupt, R.L. and S.E. Haupt, 2004: *Practical Genetic Algorithms, 2nd edition.* Wiley, New York, NY, 255 pp.

Holmes, 2006, Poster Presentation

Hsu, S.A., 2003: Nowcasting Mixing Height and Ventillation Factor for Rapid Atmospheric Dispersion Estimates on Land, *National Weather Digest,* 37, 75-78.

Long, K.J., S.E. Haupt, and G.S. Young, 2008: Optimizing Source Characteristics and Meteorological Data Describing a Contaminant Release with a Genetic Algorithm. Submitted to *Optimization and Engineering.*

Lumely, J.L., 1962: the Mathematical Nature of the Problem of relating Lagrangian and Eulerian Statistical Functions in Turbulence *Mecanique de La Turbulence,* Èd. Du Centre Nat. del la Rech. Sci., Paris, 17-26.

Lorenz, E.N., 1963: Deterministic Periodic Flow, Journal of Atmospheric Science, 20, 130-141

McMullen, R.W., 1975: The Change of Concentration Standard Deviations with Distance, JAPCA

Stull, R.B., 1988: An *Introduction to Boundary Layer Meteorology*. Kluwar Academic, The Netherlands, 666 pp.

Taylor, G.I., 1922: Diffusion by Continuous Movements *Proc. London Math Soc.* **A20** 196-212.

Weil, J.C., 1988: Dispersion in the Convective Boundary Layer. *Lectures on Air Pollution Modeling,* A. Venkatram and J.C. Wyngaard, Eds., Amer. Meter. Soc. 167-227.

Wyngaard, J.C. 2008: To be published by Cambridge University Press.